Acta Geochim (2023) 42:637–647
https://doi.org/10.1007/s11631-023-00609-7

ORIGINAL ARTICLE

Mercury accumulation, distribution, and isotopic composition in tissues of the Collared Scops Owl (*Otus lettia*)

Dongya Jia[1] · Kang Luo[2] · Zhidong Xu[2] · Xiaohang Xu[3] · Chan Li[4] · Hongmei Wu[2,5] · Dawei Wang[2,5] · Hui Ye[6] · Gaoen Wu[7] · Zhuo Chen[1] · Guangle Qiu[2]

Received: 19 February 2023 / Revised: 8 March 2023 / Accepted: 6 April 2023 / Published online: 4 May 2023

Abstract Mercury is a ubiquitous contaminant known to accumulate in wildlife, particularly bird species at higher trophic levels. Knowledge of tissue-specific Hg distributions aids our understanding of Hg bioaccumulation in organisms. In this study, one adult and three juvenile Collared Scops Owls (*Otus lettia*) were studied to elucidate the bioaccumulation of Hg in body tissues. Six tissues and organs (feathers, nails, heart, liver, gizzard, and muscle), as well as gastric contents, were examined for total Hg (THg) and methylmercury (MeHg) contents, Hg isotopic compositions including mass-dependent fractionation (MDF; δ^{202}Hg) and mass-independent fractionation (MIF; Δ^{199}Hg and Δ^{201}Hg), and C (δ^{13}C) and N (δ^{15}N) isotopic compositions. Tissue-specific THg and MeHg concentrations in the adult were in the ranges of 150–1360 ng/g and 17–1060 ng/g, and lower in the juveniles at 91–419 ng/g and 67–350 ng/g, respectively. The δ^{202}Hg values in the adult were strongly negative at $-1.75‰ \pm 0.17‰$ compared with the juveniles at $-0.99‰ \pm 0.25‰$. The adult exhibited lower MIF values than the juveniles, at $0.23‰ \pm 0.07‰$ for Δ^{199}Hg and $0.2‰ \pm 0.11‰$ for Δ^{201}Hg, compared with $0.81‰ \pm 0.09‰$ and $0.66‰ \pm 0.07‰$, respectively. The lower adult MDF and MIF values suggest that the adult tended to accumulate negative Hg isotopes but the juvenile's positive Hg isotopes. Differences between adult and juvenile tissue Hg concentrations indicate that metabolic processes play an important role in Hg accumulation.

Keywords Mercury · Methylmercury · Mass-dependent fractionation · Mass-independent fractionation · Tissue · Terrestrial bird

✉ Zhuo Chen
chenzhuo19@163.com

✉ Guangle Qiu
qiuguangle@vip.skleg.cn

[1] School of Chemistry and Materials Science, Guizhou Normal University, Guiyang 550001, China

[2] State Key Laboratory of Environmental Geochemistry, Institute of Geochemistry, Chinese Academy of Sciences, Guiyang 550081, China

[3] College of Resources and Environmental Engineering, Guizhou University, Guiyang 550025, China

[4] School of Ecology and Environmental Science, Yunnan University, Yunnan 650091, China

[5] University of Chinese Academy of Sciences, Beijing 100049, China

[6] School of Public Health, Guizhou Medical University, Guiyang 550025, China

[7] College of Ecology and Environment, Hainan University, Hainan 570228, China

1 Introduction

Mercury is commonly found in the environment and is harmful to wildlife and human health (Hall et al. 1997; Mergler et al. 2007). It exists mainly in its inorganic form in the environment but the inorganic Hg can be converted to highly neurotoxic methylmercury (MeHg) under microbial or photochemical action (Lavoie et al. 2013). MeHg has a strong bioaccumulation tendency with biomagnification in top predators, especially via aquatic food chains (Jackson et al. 2020; Li et al. 2021; Zhang et al. 2022).

It is widely accepted that bird species at the top of the food chain accumulate Hg. An increasing trend in MeHg exposure has been reported in both seabirds and terrestrial birds worldwide (Carravieri et al. 2016; Luo et al. 2020), attracting public concern (Day et al. 2012; Manceau et al. 2021a). Mercury exposure is considered a possible contributor to bird population decline (Evers et al. 2008; Ogden 1974), as verified by recent studies in the Everglades USA (Perkins et al. 2020). Mercury in food is absorbed through the gastrointestinal tract and transported and redistributed via the bloodstream to various tissues and organs (Mallory et al. 2018; Renedo et al. 2021; Tsui et al. 2018; Zolfaghari et al. 2009). Differences in detoxification strategies between bird species may cause differences in Hg accumulation (Monteiro and Furness 2001; Spalding et al. 2000).

Bird feathers and blood are important indicators of body Hg loads and habitat Hg levels. Feather Hg content is considered a reliable indicator of long-term (months) exposure and body Hg load (during the period of feather formation) (Ausems et al. 2021; Burger 1993; Furness et al. 1986; Furtado et al. 2021). Mercury stabilized in feathers during metabolism can account for up to ~ 93% of total body Hg loads and is an important pathway for Hg excretion (Braune 1987). Blood Hg acts as a short-term (days to weeks) Hg exposure indicator, reflecting recent levels of exposure and habitat Hg levels. While feather and blood samples can easily be obtained, internal tissues and organs such as the liver, kidney, muscle, and brain are typically sampled for toxicological evaluation of Hg exposure (Evers et al. 2005). Knowledge of patterns of Hg accumulation and distribution in bird tissues and organs improves our understanding of Hg body burdens and detoxification processes.

Stable C ($\delta^{13}C$) and N ($\delta^{15}N$) isotopic compositions are useful in quantifying and reconstructing diet and food-web structures, aiding our understanding of temporospatial variations in food sources and how pollutants in foods are redistributed in the body with energy flow (Hobson and Welch 1992; McCutchan Jr et al. 2003). Enrichment in ^{15}N from diet to consumer is indicated by increases in $\delta^{15}N$ values by 2.5–3.4 ‰, allowing the identification of trophic levels (Caut et al. 2008, 2009; Post 2002; Vander Zanden et al. 1997). Enrichment in ^{13}C between diet and consumer accounts for changes in $\delta^{13}C$ values of $\leq$ 1.0‰ and may be useful in tracing prey–consumer connections or food chains (DeNiro and Epstein 1978; Peterson and Fry 1987; Post 2002). Variations in metabolic rates of different tissues and organs may result in isotopic fractionation (Hobson and Clark 1992), although it remains unclear whether this affects the accumulation and redistribution of Hg in bird tissues and organs.

Non-traditional stable-isotope ratios of Hg are increasingly used to trace Hg sources and metabolic responses in biota (Blum and Bergquist 2007). Hg isotopes may undergo both mass-dependent fractionation (MDF, indicated by $\delta^{202}Hg$ values) and mass-independent fractionation (MIF, indicated by $\Delta^{199}Hg$ and $\Delta^{201}Hg$ values; Sect. 2.4) during biogeochemical processes. Isotopic composition signatures provide rich diagnostic information for the identification of sources, transformations, and metabolic processes of Hg in biological samples (Bergquist and Blum 2007; Blum et al. 2014). Recent studies have reported the characteristics of Hg isotopes in different organs of seabirds, with demethylation reactions resulting in mass fractionation (Manceau et al. 2021b; Poulin et al. 2021; Queipo-Abad et al. 2022; Renedo et al. 2021). However, Hg isotopic signatures of different tissues and organs of terrestrial birds are not fully resolved. Only a few investigations on Hg isotope compositions, particularly tissue-specific Hg isotopic signatures in terrestrial birds were available (Liu et al. 2020; Tsui et al. 2018).

In this study, total Hg (THg) and MeHg contents, $\delta^{13}C$ and $\delta^{15}N$ values, and Hg isotopic compositions ($\delta^{202}Hg$, $\Delta^{199}Hg$, and $\Delta^{201}Hg$) of six tissues/organs and gastric contents of four Collared Scops Owls (*Otus lettia*) were determined, with the aims of (1) revealing the distributions of THg, MeHg, and Hg isotopic compositions in different tissues/organs of the owls; and (2) elucidating the mechanisms of tissue-specific Hg distribution through metabolic processes.

2 Materials and methods

2.1 Study area

Jingmai Airport is a regional airport in Lancang County, southwest Yunnan Province, South China, which was selected as the sampling site (Fig. S1). It lies in the Nushan Mountain range of the Hengduan Mountains, bordering Myanmar to the west and southwest. The study region has a subtropical mountain monsoon climate with an annual rainfall of 1624 mm and an average temperature of 19.2 °C. There is ~ 54% forest cover, making it a biologically rich and diverse ecosystem.

2.2 Sample collection and preparation

The Collared Scops Owl is a small raptor widely distributed in Yunnan Province. It feeds mainly on grasshoppers, locusts, beetles, and other insects (https://www.owlpages.com/owls/species.php?s=750). It prefers to perch in open areas, as provided by the airport environment. Many owls are caught in fog nets around the airport

each year, with most being released safely. In 2021, four owls (one adult and three juveniles) were found dead in the airport perimeter fog net, and these were collected and stored in a refrigerator at –20 °C.

The owls were dissected and external tissues (chest feathers and nails), internal tissues/organs (heart, liver, gizzard, muscles), and gastric contents were collected. The 24 samples of tissues/organs were thoroughly cleaned with Milli-Q ultrapure water, lyophilized, and ground into powder (200 mesh) for analysis. The four samples of gastric contents were lyophilized after the removal of sand and stones, and ground to powder.

Sample collection was approved by the administrative office of Jingmai Airport, and the State Key Laboratory of Environmental Geochemistry, Institute of Geochemistry, Chinese Academy of Sciences.

2.3 Mercury analysis

Due to the small mass of each tissue sample, acid digestion methods were applied in both THg and MeHg analyses (Hammerschmidt and Fitzgerald 2005; Tsui et al. 2018).

Feather (5–10 mg) and other (200–500 mg) samples were weighed into pre-cleaned Teflon vessels; 5 mL 4.6 mol/L HNO_3 was added, and the mixture was digested at 60 °C for ~ 20 h. The mixtures were shaken every 2 h during digestion to ensure sufficient reaction. After digestion, ~ 1 mL of solution was taken for MeHg determination; 5 mL concentrated HNO_3 was added to the remaining solution, and digestion continued for 3 h at 95 °C. After cooling, 400 μL BrCl solution was added, and the solution was diluted to 25 mL after a further 24 h for THg determination.

For THg determination, hydroxylamine hydrochloride was added to ~ 4 mL of digestate to neutralize excess BrCl before an appropriate aliquot was placed in a bubbler tube for analysis by $SnCl_2$ reduction and cold-vapor atomic fluorescence spectrometry (CVAFS; Brooks Rand Model III, USA) following US Environmental Protection Agency Method 1631E (USEPA 2002). For MeHg determination, ~ 50 μL of digestate was placed in a bubbler with acetic acid–sodium acetate buffer solution for aqueous ethylation, Tenax trap (SUPELCO, USA) collection, gas chromatographic separation, and CVAFS analysis following USEPA Method 1630 (USEPA 2001). All results are reported on a dry-weight basis.

Quality control and assurance (QA/QC) procedures included analysis of blanks, duplicates, and reference materials (GBW 0901b and TORT2). GBW 0901b (human hair, Shanghai Institute of Applied Physics, Chinese Academy of Sciences, Shanghai, China) was used for THg analyses and TORT2 (lobster pancreas, National Research Council Canada) for MeHg analyses. The specific results are shown in Table S1. Duplicate analyses were undertaken for 10% of the samples. Recoveries of THg and MeHg were 87 ± 8.4 % and 94 ± 9.1 %, respectively, with relative standard deviations of < 20% for both sets of results. For THg, the TORT2 certified value is 270 ± 60 ng/g, the measured value is 237 ± 32 ng/g (n = 7), and the human hair certified value is 1060 ± 280 ng/g, the measured value is 1010 ± 160 ng/g (n = 4). Our measured values were no significant difference with certified at the 95% confidence level. For MeHg, the TORT-certified value is 152 ± 13 ng/g, the measured value is 142 ± 14 ng/g. The slightly low measured value may be due to changes in the sensitivity of the instrument to the environment (Azemard and Vassileva 2015, 2021).

2.4 Hg isotopic composition

Hg isotopic analyses were undertaken at the State Key Laboratory of Environmental Geochemistry (SKLEG), Institute of Geochemistry, Chinese Academy of Sciences, Guiyang, China, using a Neptune Plus multicollector–inductively coupled plasma–mass spectrometry system (Thermo Fisher Scientific, Germany) equipped with a continuous-flow injection system. Isotopic compositions are expressed as per mil (‰). US National Institute of Standards and Technology (NIST) standard reference material (SRM) 3133 solution matching the THg concentration and solution acidity was analysed before and after each sample. The instrumental error was corrected using NIST SRM 997 TL throughout the process. The injection system was cleaned with 5% HNO_3 between samples to eliminate interference.

The δ^{202}Hg (MDF), and Δ^{199}Hg and Δ^{201}Hg (MIF) values were calculated as follows (Bergquist and Blum 2007):

$$\delta^{202}\mathrm{Hg} = 1000 \times \left[\left(\delta^{202}\mathrm{Hg} / \delta^{198}\mathrm{Hg}\right)_{\mathrm{Sample}} / \left(\delta^{202}\mathrm{Hg} / \delta^{198}\mathrm{Hg}\right)_{\mathrm{NIST3133}}\right) - 1\right]‰ \quad (1)$$

$$\Delta^{199}\mathrm{Hg} \approx \delta^{199}\mathrm{Hg} - \left(\delta^{202}\mathrm{Hg} \times 0.2520\right) \quad (2)$$

$$\Delta^{201}\mathrm{Hg} \approx \delta^{201}\mathrm{Hg} - \left(\delta^{202}\mathrm{Hg} \times 0.7520\right) \quad (3)$$

NIST SRM 8610 (UM-Almadén) was used as a second standard with analysis after every seven samples. The measured values (δ^{202}Hg = − 0.53 ± 0.05 ‰, Δ^{199}Hg = − 0.04 ± 0.04 ‰, 2 SD) were consistent with those reported by (Bergquist and Blum 2007). Certificated reference materials BCR-482 (epiphytic lichen) and TORT3 (lobster hepatopancreas, Canada) were analysed as samples to assess result accuracy. The measured values (δ^{202}Hg = − 1.54 ± 0.09 ‰, Δ^{199}Hg = − 0.60 ± 0.03 ‰,

2SD, n = 3) for BCR-482, and (δ^{202}Hg = − 0.71 ± 0.03‰, Δ^{199}Hg = 0.77 ± 0.07 ‰, n = 1) for TORT3 were consistent with previously reported values (Kwon et al. 2014; Li et al. 2020; Liu et al. 2020; Renedo et al. 2018).

2.5 C and N isotopic compositions

C and N isotopic analyses were undertaken at the SKLEG with samples of ~ 0.1 and ~ 0.5 mg, respectively. Cellulose and Caffeine (International Atomic Energy Agency (IAEA-C_3: δ^{13}C = –24.7 ± 0.04‰, and IAEA-600: δ^{13}C = –27.7 ± 0.07 ‰), and $(NH_4)_2SO_4$ (IAEA-N_1: δ^{15}N = 0.4 ± 0.06 ‰) were used as standards for C and N isotopic analyses. Analyses involved an EA 2000 elemental analyser and a MAT 253 isotope ratio mass spectrometer (both from Thermo Fisher Scientific, Germany). The δ values were calculated as follows:

$$X = (R_{Sample} - R_{Standard} - 1) \times 1000‰ \quad (4)$$

where X is ^{15}N or ^{13}C, and R_{Sample} and $R_{Standard}$ are the N and C isotopic abundance ratios of sample and standards (i.e., ^{15}N/^{14}N and ^{13}C/^{12}C, respectively). Vienna Pee Dee Belemnite (V-PDB) and atmospheric nitrogen were used as reference standards.

2.6 Statistical analysis

Excel 2021 (Microsoft Corp., USA) was used for calculations, and Origin Pro2022b (OriginLab Corp., USA) for plotting and statistical analysis.

3 Results and discussion

3.1 C and N isotopic compositions

The δ^{13}C values in owl tissues ranged from –29.31 to –22.95 ‰, with average values of –24.99 ± 1.40 ‰ in juveniles and –26.28 ± 1.92 ‰ in the adult. Both the adult and juveniles had the highest δ^{13}C values in feathers. Except for the liver of the adult, internal organs had δ^{13}C values lower than those of external tissues. Gastric contents of juveniles and adults had δ^{13}C values ranging from –27.65 ‰ (juvenile) to –26.88 ‰ (adult).

There was a wide range of δ^{15}N values in different tissues of 2.43–8.13‰, with a higher average value in the adult (5.92 ± 1.12 ‰) than in the juveniles (3.75 ± 1.00 ‰) (Fig. 1, Fig. S2, Table S2). The higher adult value is consistent with its higher trophic position. As for δ^{13}C values, both the adult and juveniles had the highest δ^{15}N values in feathers and the lowest in muscles. δ^{15}N values were low (1.70–4.02 ‰) in the gastric contents of both the adult and juveniles, indicating a predator–prey fractionation effect.

3.2 Hg in tissues

THg and MeHg contents of tissues/organs of the adult were in the ranges of 150–1360 and 120–1060 ng/g, respectively. The highest average values were recorded in feathers and nails: 1090 ± 190 and 1360 ± 67 ng/g for THg, and 960 ± 42 and 1060 ± 54 ng/g for MeHg, respectively. Muscle and gizzard tissues had the lowest average values of 160 ± 4 and 150 ± 9 ng/g for THg, and 140 ± 12 and 120 ± 1 ng/g for MeHg, respectively. For juveniles, THg and MeHg contents of tissues/organs were in ranges of 91–420 and 67–350 ng/g, respectively, with the highest average values in feathers and nails of 310 ± 37 and 360 ± 76 ng/g for THg, and 280 ± 50 and 250 ± 74 ng/g for MeHg, respectively. Muscle and gizzard tissues again had the lowest values, with averages of 110 ± 17 and 120 ± 18 ng/g for THg, and 87 ± 13 and 94 ± 23 ng/g for MeHg, respectively (Figs. 2a, b).

MeHg/THg ratios (MeHg%) of all tissues and organs for both the adult and juveniles were in the range of 59.6–96.2 %, indicating the predominant MeHg form. As a typical MeHg detoxification organ, the liver was also characterized by high MeHg ratios with averages of 73.5 ± 4.0 % for the adult and 80.45 ± 8.9 % for juveniles, possibly indicating heavier MeHg exposure in the latter.

There were notable differences between the adult and juveniles in THg and MeHg contents of feathers and nails (Figs. 2c, d). The average THg and MeHg contents of feathers of the adult were higher than those of juveniles by factors of 3.5 and 3.4, respectively. The average THg and MeHg contents of the nails of the adult were also higher than those of juveniles, by factors of 3.8 and 4.3, respectively. In contrast, there were no major differences between the adult and juveniles in THg and MeHg contents of the heart, liver, gizzard, or muscle. These results are consistent with the adult and juvenile Buzzard (*Buteo buteo*) in Scotland (Lancaster et al. 2022) and Razorbirds (*Alca torda*) in Spain (Espin et al. 2012), which were no significant differences in the internal organization of adult and juvenile birds.

Feathers and nails comprise mainly keratin, a protein comprising amino acids with high contents of sulfhydryl groups that readily combine with Hg. When combined with keratin, Hg becomes inert (Rouse and Van Dyke 2010), and this process is considered an important pathway for Hg excretion in birds. Gastric contents of both the adult and juveniles had average THg contents and MeHg% values of 65–105 ng/g and 35.3 ± 6.7%, respectively, with the marked difference between the adult and juveniles in THg

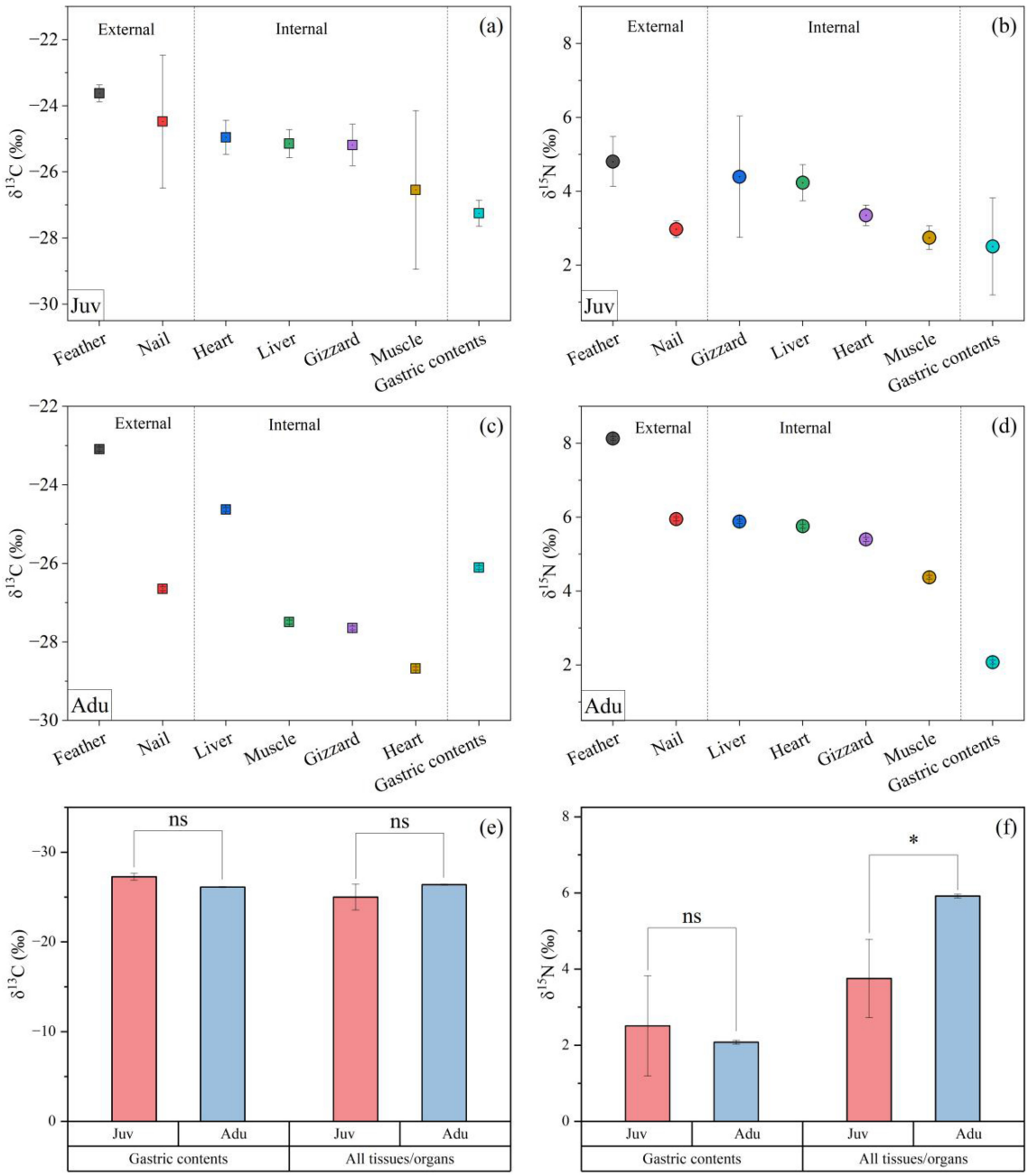

Fig. 1 Tissue-specific $\delta^{13}C$ and $\delta^{15}N$ values in the adult and juvenile owls. Figures a and c are plotted every tissue-specific $\delta^{13}C$ in juveniles' mean value and adult value, respectively, and Figures b and d are plotted every tissue-specific $\delta^{15}N$ in juveniles' mean value and adult value, respectively. Figure e shows a comparison of $\delta^{13}C$ of gastric contents and tissues/organs in juveniles and adults. Figure f shows a comparison of $\delta^{15}N$ of gastric contents and tissues/organs in juveniles and adults

and MeHg contents reflecting their different exposure periods and Hg metabolic processes (Figs. 2a, b).

3.3 Hg isotopic composition

Average tissue/organ $\delta^{202}Hg$ values for the adult and juveniles were within the ranges of –1.95‰ to –1.44‰ and –1.18‰ to –0.77‰, respectively, while individual tissue/organ values tended to be more negative in the former (Fig. 3a). Nails had the highest $\delta^{202}Hg$ values, and feathers and the liver had the lowest. The $\delta^{202}Hg$ values of tissues/organs (barring muscle) differed by a uniform factor of 2 between the adult and juveniles, likely reflecting differences in metabolism.

Tissues/organs of the adult had similar $\Delta^{199}Hg$ and $\Delta^{201}Hg$ values, as did those of the juveniles, but values

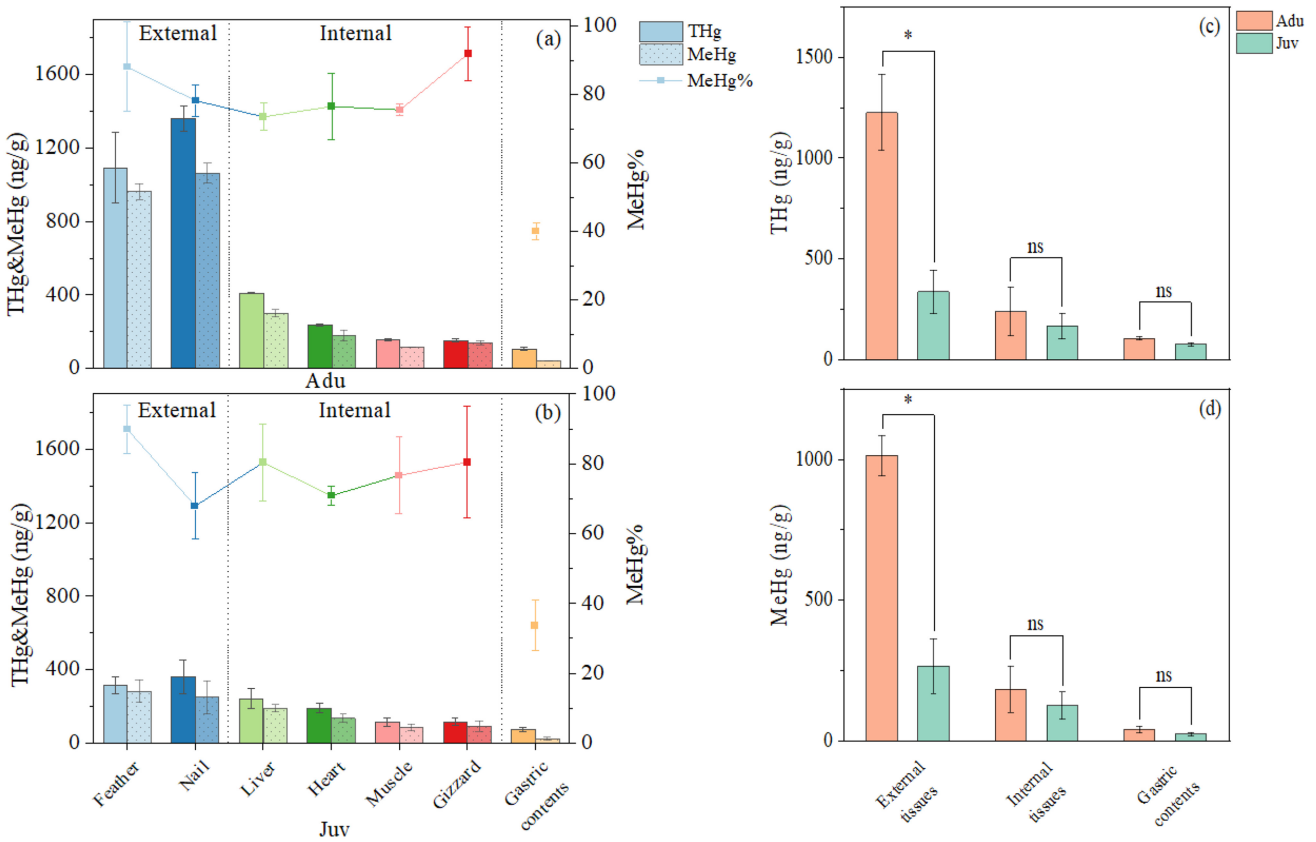

Fig. 2 Comparison of THg and MeHg contents of tissues/organs between the adult and juvenile owls

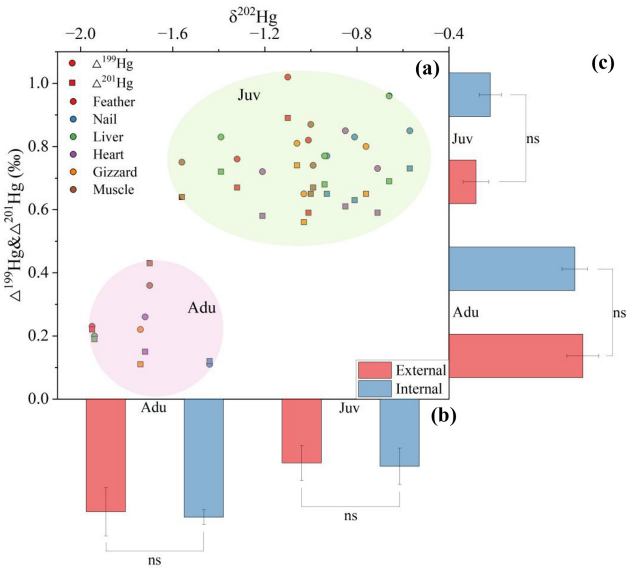

Fig. 3 δ^{202}Hg–Δ^{199}Hg plots for juvenile and adult owls. Figure a is plotted according to the values of MDF and MIF. MIF (Δ^{199}Hg) is represented by circle, but MIF (Δ^{201}Hg) is represented by square. Figures b and c are plotted according to the mean value of internal (heart, liver, gizzard, and muscle) and external (feather, nail) tissue sites of MDF and MIF(Δ^{199}Hg), respectively. Readers can distinguish different tissues/organs of the owl in the supplementary parts of the article only in the web version

were higher overall in the latter (Fig. 3a), with average ranges of 0.11–0.36 ‰ and 0.11–0.43 ‰ in the adult and 0.75–0.86 ‰ and 0.59–0.72 ‰ in juveniles, respectively. The similarity of MIF values between tissues and organs of both the adult and juveniles indicates that metabolic processes had little fractionation effect, implying homogenous food sources (Figs. 3b, c). However, MDF and MIF values were markedly different between the adult and juveniles, by factors of 1.7 for δ^{202}Hg and 4 for Δ^{199}Hg.

Metabolic processes involve blood circulation and constant exchange with blood in organs, so no marked differences were observed among tissues/organs for Hg contents or MDF, MIF, δ^{13}C, and δ^{15}N values. There was a slight variation in MDF values between external and internal tissues, with feathers accumulating lighter Hg isotopes than internal tissues, and nails heavier isotopes. Feather MDF values were ~ 0.9 times those of internal tissues, and nails ~ 1.2 times.

Relationships between tissue-specific δ^{202}Hg and respective δ^{13}C and δ^{15}N values of the adult and juvenile owls are shown in Fig. 4. MDF values are negatively correlated with δ^{15}N and δ^{13}C values in tissues and organs of the adult, and positive in juveniles. Due to the similarity of MIF values among tissues and organs of both the adult and juveniles, there was no significant correlation between

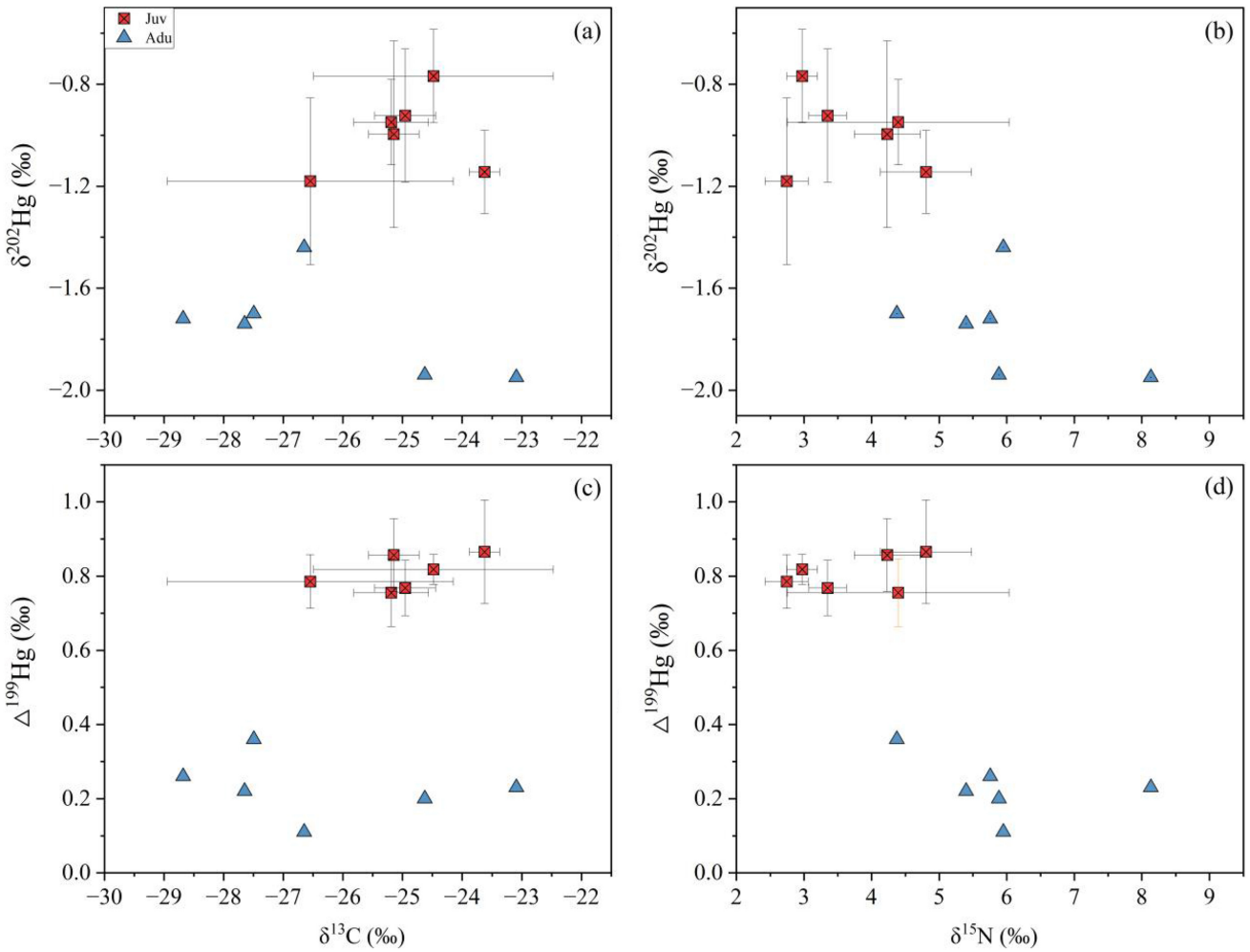

Fig. 4 Hg Δ^{199}Hg and Δ^{201}Hg values relative to δ^{13}C and δ^{15}N values. Squares and triangles represent tissues/organs from juvenile and adult owls, respectively. The juvenile birds were presented with mean and standard deviation prevention

Δ^{199}Hg and δ^{15}N or δ^{13}C values. These MDF distribution patterns between adult and juvenile owls indicate the possible utility of MDF in determining the growth stage of birds.

The Δ^{199}Hg/Δ^{201}Hg ratios indicate photochemical processes of MeHg photodemethylation and Hg (II) photoreduction, characterized by ratios of 1.36 ± 0.02 and 1.00 ± 0.01, respectively (Bergquist and Blum 2007). The juveniles have slightly higher ratios than the adult (Fig. 5), with a ratio of 1.21 in the former indicating more MeHg photodegradation, while the adult ratio of 1.00 may be attributed to the photoreduction of Hg (II).

The positive MDF values of juveniles suggest they tended to accumulate the heavier Hg isotope, while the negative values of the adult indicate the accumulation of the lighter isotope. The marked difference in THg content between adult and juvenile feathers and nails, the main

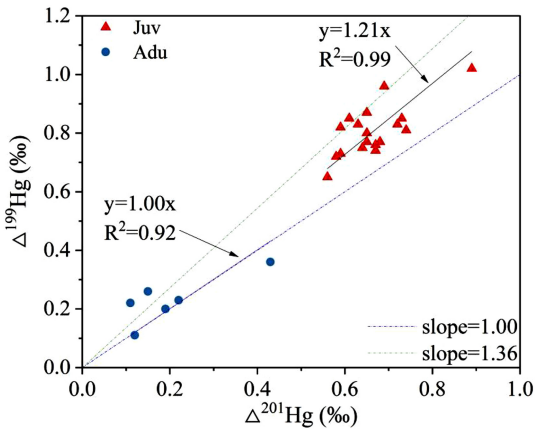

Fig. 5 Δ^{199}Hg–Δ^{201}Hg plots for the adult and juvenile owls and theoretical photodemethylation and photoreduction trends (Bergquist and Blum 2007)

Table 1 MDF and MIF values of tissues in seabirds and terrestrial birds

Tissue	Species	THg (ng/g)	δ^{202}Hg(‰)	Δ^{199}Hg (‰)	Refs.
Terrestrial birds					
Blood	Vireo	340–540	−0.84 to −0.34	0.83 to 1.12	Tsui et al. (2018)
	Yellowthroat	230.8–879.6	−1.56 to −1.1	0.06 to 0.44	
	Thrush	133–358	−1.95 to −0.08	0.48 to 1.31	
	Vireo	336–480	−1.43 to −0.39	0.55 to 1.01	
Feather	Buzzards	15.8–98.4	−1.69 to 0.00	1.87 to 2.72	Liu et al. (2020)
	Owl	508 ± 339	−1.95 to −1.01	0.23 to 1.02	This study
Gizzard	Owl	125.21 ± 22.08	−1.74 to −0.76	0.22 to 0.81	
Heart	Owl	202.88 ± 25.4	−1.72 to −0.71	0.26 to 0.85	
Liver	Owl	284.87 ± 80.94	−1.94 to −0.66	0.20 to 0.96	
Muscle	Buzzards	15.8–45.9	−1.77 to −0.69	1.51 to 2.89	Liu et al. (2020)
	Owl	125 ± 23	−1.70 to −0.99	0.36 to 0.87	This study
Nail	Owl	610.49 ± 437.57	−1.44 to −0.57	0.11 to 0.85	
Seabirds					
Feather	Prion	1220–3980	1.19 to 1.55	2.21 to 2.52	Renedo et al. (2021)
	Auks	810–4530	−0.24 to 1.43	0.14 to 1.91	
	Petrel	8500–21,200	2.31 to 2.35	1.24 to 1.34	
	Petrel	3010–8540	0.91 to 1.31	1.26 to 1.71	
	Petrel	4800–26,200	2.57 to 3.05	1.4 to 1.75	Manceau et al. (2021b)
	Penguin	290–530	0.48 to 0.89	1.62 to 2.02	Renedo et al. (2018)
	Skua	1340–2390	0.08 to 0.51	1.32 to 1.57	
	Penguin	1060–1690	2.15 to 2.51	1.95 to 2.2	
	Penguin	1550–7590	1.31 to 1.68	1.33 to 1.66	
	Penguin	1660–4140	1.7 to 2.15	1.66 to 1.96	
	Penguin	1850–2570	1.76 to 2.26	1.66 to 1.94	
	Penguin	1250–2030	2.26 to 2.68	2.08 to 2.36	
	Skua	2290–17,670	0.93 to 1.72	1.32 to 1.82	
Liver	Prion	1490–2520	−0.28 to 0.3	1.84 to 1.98	Renedo et al. (2021)
	Petrel	214,200–405,200	−0.28 to 0.68	1.23 to 1.34	
	Petrel	30,650–81,000	−0.99 to −0.11	1.05 to 1.23	
	Petrel	1110–932,840	−1.48 to 0.14	1.06 to 1.44	Queipo-Abad et al. (2022)
	Petrel	170,000–1,499,000	−0.1 to 1.87	1.3 to 1.67	Manceau et al. (2021b)
	Grebe	43,100	−2.07 to −0.17	1.42 to 1.49	Poulin et al. (2021)
	Tern	13,800	−0.14 to 0.45	0.67 to 0.71	
	Skua	8190	0.8	2.02	
Muscle	Prion	230–430	−0.19 to 0.89	1.77 to 2.16	Renedo et al. (2021)
	Petrel	1660–29,200	0.38 to 0.55	1.28 to 1.41	
	Petrel	2230–7810	−0.17 to 0.6	1.1 to 1.37	
	Petrel	2870–88,700	−1.19 to 2.78	1.36 to 1.97	Manceau et al. (2021b)
	Grebe	7100	−1.13 to −0.22	1.43 to 1.46	Poulin et al. (2021)
	Tern	6390	0.31 to 0.53	0.72 to 0.79	
	Skua	1750	1.25 to 1.25	1.99 to 1.99	
	Petrel	110–52,270	−0.98 to 1.25	0.89 to 1.73	Queipo-Abad et al. (2022)

pathway of Hg excretion in birds, and the tissue-specific Hg isotopic composition pattern between juveniles and the adult insinuate changes in Hg metabolism during different life stages of the owl. This result is like that of the Hermit Thrush in the US, where after the hatching year bird's MDF and MIF were both slightly above the mean of the second year and after second year birds (Tsui et al. 2018).

Average $\delta^{13}C$ and $\delta^{15}N$ values and THg and MeHg contents of the gastric contents of juveniles were like those of the adults (Figs. 1, 2, S3), indicating a similar diet. The difference in tissue/organ THg and MeHg contents between adults and juveniles is therefore unlikely to reflect their food sources. Juveniles have a shorter predation and accumulation/detoxification period, which may explain their more positive MDF and MIF values. Considering the significant differences between adults and juveniles in terms of the Hg contents of feathers and nails, metabolic processes play an important role in Hg accumulation.

Few data have been reported for Hg isotopes in terrestrial birds (Tsui et al. 2018; Liu et al. 2020). MDF and MIF values of the owls studied here lie within the range for terrestrial birds, MDF of terrestrial birds have negative values while seabirds have positive values (Table 1), but the MIF values are significantly lower than those observed in vultures (*Aegypius monachus*) collected from the Tibetan Plateau, China (Table 1), for which higher Hg contents and more positive MDF and MIF tissue/organ values were reported relative to other terrestrial birds. High tissue/organ Hg contents seem to be associated with more positive (higher) MDF values, consistent with the accumulation of the heavier Hg isotope.

4 Conclusions

This study elucidated the accumulation, distribution, and isotopic composition of Hg in six different tissues/organs of the Collared Scops Owl. There are marked differences in the Hg content of feathers and nails between adult and juvenile owls. The adult sample had lower MDF and MIF values than the juveniles, indicating the accumulation of negative Hg isotopes. This isotopic pattern reflects changes in Hg metabolism during different life stages of the owl. We must point out that the number of individuals was limited, and a more extensive study is required to verify the significance of differences in Hg isotopic composition between adults and juveniles of this bird species.

Supplementary Information The online version contains supplementary material available at https://doi.org/10.1007/s11631-023-00609-7.

Acknowledgements This work was supported by National Natural Science Foundation of China (NSFC No. 42103080). We thank Jingmai Airport staff for their assisstance in sample collection and thank Dr. Jialiang Han, Fudong Zhang, Yuxiao Shao and others for their help during the experiment.

Author contributions DJ: Conceptualization, investigation, visualization, methodology, formal analysis, writing—original draft, writing—review and editing. KL: investigation, methodology, writing—review and editing. ZX: investigation, formal analysis, writing—review and editing. XX: validation, writing—review and editing. CL: methodology, investigation, resources. HW: methodology, investigation, resources. DW: methodology, investigation, resources. HY: resources, writing—review and editing. GW: resources, writing—review and editing. ZC: resources, funding acquisition, writing—review and editing. GQ: supervision, formal analysis, funding acquisition, writing—review and editing.

Declarations

Conflict of interest On behalf of all authors, the corresponding author states that there is no conflict of interest.

Ethical approval Sample collection was approved by the administrative office of Jingmai Airport, and the State Key Laboratory of Environmental Geochemistry, Institute of Geochemistry, Chinese Academy of Sciences. The dissection was approved by the Animal Care Welfare Committee of Guizhou Medical University (No.2100345).

References

Ausems A, Skrzypek G, Wojczulanis-Jakubas K, Jakubas D (2021) Birds of a feather moult together: differences in moulting distribution of four species of storm-petrels. PLOS One. 16:e0245756. https://doi.org/10.1371/journal.pone.0245756

Azemard S, Vassileva E (2015) Determination of methylmercury in marine biota samples with advanced mercury analyzer: method validation. Food Chem 176:367–375. https://doi.org/10.1016/j.foodchem.2014.12.085

Azemard S, Vassileva E (2021) Rapid determination of femtomolar methylmercury in seawater using automated GC-AFS method: optimisation of the extraction step and method validation. Talanta 232:122492. https://doi.org/10.1016/j.talanta.2021.122492

Bergquist BA, Blum JD (2007) Mass-dependent and -independent fractionation of hg isotopes by photoreduction in aquatic systems. Science 318:417–420. https://doi.org/10.1126/science.1148050

Blum JD, Bergquist BA (2007) Reporting of variations in the natural isotopic composition of mercury. Anal Bioanal Chem 388:353–359. https://doi.org/10.1007/s00216-007-1236-9

Blum JD, Sherman LS, Johnson MW (2014) Mercury isotopes in earth and environmental sciences. Annu Rev Earth Planet Sci 42:249. https://doi.org/10.1146/annurev-earth-050212-124107

Braune BM (1987) Comparison of total mercury levels in relation to diet and molt for nine species of marine birds. Arch Environ Contam Toxicol 16:217. https://doi.org/10.1007/BF01055802

Burger J (1993) Metals in avian feathers: bioindicators of environmental pollution. Rev Environ Toxicol 5:197–306

Carravieri A, Cherel Y, Jaeger A, Churlaud C, Bustamante P (2016) Penguins as bioindicators of mercury contamination in the southern Indian Ocean: geographical and temporal trends. Environ Pollut 213:195. https://doi.org/10.1016/j.scitotenv.2013.02.060

Caut S, Angulo E, Courchamp F (2008) Avoiding surprise effects on Surprise Island: alien species control in a multitrophic level perspective. Biol Invasions 11:1689–1703. https://doi.org/10.1007/s10530-008-9397-9

Caut S, Angulo E, Courchamp F (2009) Variation in discrimination factors ($\Delta^{15}N$ and $\Delta^{13}C$): the effect of diet isotopic values and applications for diet reconstruction. J Appl Ecol 46:443–453. https://doi.org/10.1111/j.1365-2664.2009.01620.x

Day RD, Roseneau DG, Berail S, Hobson KA, Donard OF, Vander Pol SS et al (2012) Mercury stable isotopes in seabird eggs

reflect a gradient from terrestrial geogenic to oceanic mercury reservoirs. Environ Sci Technol 46:5327–5335. https://doi.org/10.1021/es2047156

DeNiro MJ, Epstein S (1978) Influence of diet on the distribution of carbon isotopes in animals. Geochim Cosmochim Acta 42:495–506. https://doi.org/10.1016/0016-7037(78)90199-0

Espín S, Martínez-López E, Gómez-Ramírez P et al (2012) Razorbills (*Alca torda*) as bioindicators of mercury pollution in the southwestern Mediterranean. Mar Pollut Bull 64:2461–2470. https://doi.org/10.1016/j.marpolbul.2012.07.045

Evers DC, Burgess NM, Champoux L, Hoskins B, Major A, Goodale WM et al (2005) Patterns and interpretation of mercury exposure in freshwater avian communities in northeastern North America. Ecotoxicology 14:193–221. https://doi.org/10.1007/s10646-004-6269-7

Evers DC, Savoy LJ, DeSorbo CR, Yates DE, Hanson W, Taylor KM et al (2008) Adverse effects from environmental mercury loads on breeding common loons. Ecotoxicology 17:69–81. https://doi.org/10.1007/s10646-007-0168-7

Furness RW, Muirhead SJ, Woodburn M (1986) Using bird feathers to measure mercury in the environment: relationships between mercury content and moult. Mar Pollut Bull 17:27. https://doi.org/10.1016/0025-326X(86)90801-5

Furtado R, Granadeiro JP, Gatt MC, Rounds R, Horikoshi K, Paiva VH et al (2021) Monitoring of mercury in the mesopelagic domain of the Pacific and Atlantic oceans using body feathers of Bulwer's petrel as a bioindicator. Sci Total Environ 775:145796. https://doi.org/10.1016/j.scitotenv.2021.145796

Hall BD, Bodaly RA, Fudge R, Rudd J, Rosenberg DM (1997) Food as the dominant pathway of methylmercury uptake by fish. Water Air Soil Pollut 100:13–24. https://doi.org/10.1023/A:1018071406537

Hammerschmidt CR, Fitzgerald WF (2005) Methylmercury in mosquitoes related to atmospheric mercury deposition and contamination. Environ Sci Technol 39:3034–3039. https://doi.org/10.1021/es0485107

Hobson KA, Clark RG (1992) Assessing avian diets using stable isotopes I: turnover of ^{13}C in tissues. The Condor 94:181–188. https://doi.org/10.2307/1368807

Hobson KA, Welch HE (1992) Determination of trophic relationships within a high Arctic marine food web using $\delta^{13}C$ and $\delta^{15}N$ analysis. Mar Ecol Prog Ser 84:9–18. https://doi.org/10.3354/meps084009

Jackson AK, Eagles-Smith CA, Emery C (2020) Spatial variation in aquatic invertebrate and riparian songbird mercury exposure across a river-reservoir system with a legacy of mercury contamination. Ecotoxicology 29:1195–1204. https://doi.org/10.1007/s10646-019-02043-z

Kwon SY, Blum JD, Chen CY, Meattey DE, Mason RP (2014) Mercury isotope study of sources and exposure pathways of methylmercury in estuarine food webs in the Northeastern U.S. Environ Sci Technol 48:10089–10097. https://doi.org/10.1021/es5020554

Lancaster ST, Peniche G, Alzahrani A et al (2022) Mercury speciation in Scottish raptors reveals high proportions of inorganic mercury in Scottish golden eagles (*Aquila chrysaetos*): Potential occurrence of mercury selenide nanoparticles. Sci Total Environ 829:154557. https://doi.org/10.1016/j.scitotenv.2022.154557

Lavoie RA, Jardine TD, Chumchal MM, Kidd KA, Campbell LM (2013) Biomagnification of mercury in aquatic food webs: a worldwide meta-analysis. Environ Sci Technol 47:13385–13394. https://doi.org/10.1021/es403103t

Li P, Yin R, Du B, Qin C, Li B, Chan HM et al (2020) Kinetics and metabolism of mercury in rats fed with mercury contaminated rice using mass balance and mercury isotope approach. Sci Total Environ 736:139687. https://doi.org/10.1016/j.scitotenv.2020.139687

Li C, Xu Z, Luo K, Chen Z, Xu X, Xu C et al (2021) Biomagnification and trophic transfer of total mercury and methylmercury in a sub-tropical montane forest food web, southwest China. Chemosphere 277:130371. https://doi.org/10.1016/j.chemosphere.2021.130371

Liu HW, Yu B, Yang L, Wang LL, Fu JJ, Liang Y et al (2020) Terrestrial mercury transformation in the Tibetan Plateau: new evidence from stable isotopes in upland buzzards. J Hazard Mater 400:123211. https://doi.org/10.1016/j.jhazmat.2020.123211

Luo K, Xu ZD, Wang X, Quan RC, Lu ZY, Bi WQ et al (2020) Terrestrial methylmercury bioaccumulation in a pine forest food chain revealed by live nest videography observations and nitrogen isotopes. Environ Pollut 263:114530. https://doi.org/10.1016/j.envpol.2020.114530

Mallory ML, Provencher JF, Robertson GJ, Braune BM, Holland ER, Klapstein S et al (2018) Mercury concentrations in blood, brain and muscle tissues of coastal and pelagic birds from northeastern Canada. Ecotoxicol Environ Saf 157:424–430. https://doi.org/10.1016/j.ecoenv.2018.04.004

Manceau A, Bourdineaud JP, Oliveira RB, Sarrazin SLF, Krabbenhoft DP, Eagles-Smith CA et al (2021a) Demethylation of methylmercury in bird, fish, and earthworm. Environ Sci Technol 55:1527–1534. https://doi.org/10.1021/acs.est.0c04948

Manceau A, Brossier R, Janssen SE, Rosera TJ, Krabbenhoft DP, Cherel Y et al (2021b) Mercury isotope fractionation by internal demethylation and biomineralization reactions in seabirds: implications for environmental mercury science. Environ Sci Technol 55:13942–13952. https://doi.org/10.1021/acs.est.1c04388

McCutchan JH Jr, Lewis WM Jr, Kendall C, McGrath CC (2003) Variation in trophic shift for stable isotope ratios of carbon, nitrogen, and sulfur. Oikos 102:378–390. https://doi.org/10.1034/j.1600-0706.2003.12098.x

Mergler D, Anderson HA, Chan LH, Mahaffey KR, Murray M, Sakamoto M et al (2007) Methylmercury exposure and health effects in humans: a worldwide concern. Ambio 36:3–11. https://doi.org/10.1579/0044-7447(2007)36[3:meahei]2.0.co;2

Monteiro LR, Furness RW (2001) Kinetics, dose−response, and excretion of methylmercury in free-living adult Cory's shearwaters. Environ Sci Technol 35:739–746. https://doi.org/10.1021/es000114a

Ogden JC, Robertson JW, Davis GE, Schmidt TW (1974) Pesticides, polychlorinated biphenols and heavy metals in upper food chain levels, everglades national park and vicinity. In: Natl Park Serv Manage Rep National Technical Information Service, editor. U.S. Department of Commerce, Washington, D.C

Perkins M, Lane OP, Evers DC, Sauer A, Adams EM, O'Driscoll NJ et al (2020) Historical patterns in mercury exposure for North American songbirds. Ecotoxicology 29:1161–1173. https://doi.org/10.1007/s10646-019-02054-w

Peterson BJ, Fry B (1987) Stable isotopes in ecosystem studies. Annu Rev Ecol Syst 18:293–320. https://doi.org/10.1146/annurev.es.18.110187.001453

Post DM (2002) Using stable isotopes to estimate trophic position: models, methods, and assumptions. Ecology 83:703–718. https://doi.org/10.1890/0012-9658(2002)083[0703:Usitet]2.0.Co;2

Poulin BA, Janssen SE, Rosera TJ, Krabbenhoft DP, Eagles-Smith CA, Ackerman JT et al (2021) Isotope fractionation from in vivo methylmercury detoxification in waterbirds. Acs Earth Space Chem 5:990–997. https://doi.org/10.1021/acsearthspacechem.1c00051

Queipo-Abad S, Pedrero Z, Marchan-Moreno C, El Hanafi K, Berail S, Corns WT et al (2022) New insights into the biomineralization

of mercury selenide nanoparticles through stable isotope analysis in giant petrel tissues. J Hazard Mater 425:127922. https://doi.org/10.1016/j.jhazmat.2021.127922

Renedo M, Amouroux D, Duval B, Carravieri A, Tessier E, Barre J et al (2018) Seabird tissues as efficient biomonitoring tools for hg isotopic investigations: implications of using blood and feathers from chicks and adults. Environ Sci Technol 52:4227–4234. https://doi.org/10.1021/acs.est.8b00422

Renedo M, Pedrero Z, Amouroux D, Cherel Y, Bustamante P (2021) Mercury isotopes of key tissues document mercury metabolic processes in seabirds. Chemosphere. 263:127777. https://doi.org/10.1016/j.chemosphere.2020.127777

Rouse JG, Van Dyke ME (2010) A review of keratin-based biomaterials for biomedical applications. Materials 3:999–1014. https://doi.org/10.3390/ma3020999

Spalding MG, Frederick PC, McGill HC, Bouton SN, McDowell LR (2000) Methylmercury accumulation in tissues and its effects on growth and appetite in captive great egrets. J Wildl Dis 36:411–422. https://doi.org/10.7589/0090-3558-36.3.411

Tsui MT, Adams EM, Jackson AK, Evers DC, Blum JD, Balogh SJ (2018) Understanding sources of methylmercury in songbirds with stable mercury isotopes: challenges and future directions. Environ Toxicol Chem 37:166–174. https://doi.org/10.1002/etc.3941

USEPA (2001) Method 1630: Methylmercury in Water by Distillation, Aqueous Ethylation, Purge and Trap, and CVAFS. In: EPA US, editor. U.S. EPA, Washington D.C., pp. pp.1–33.

USEPA (2002) Method 1631e: Mercury in Water by Oxidation, Purge and Trap, and Cold Vapor Atomic Fluorescence Spectrometry. U.S. EPA, Washington D.C., , pp. pp.1–38.

Vander Zanden MJ, Cabana G, Rasmussen JB (1997) Comparing trophic position of freshwater fish calculated using stable nitrogen isotope ratios ($\delta^{15}N$) and literature dietary data. Can J Fish Aquat Sci 54:1142–1158. https://doi.org/10.1139/f97-016

Zhang F, Xu Z, Xu X, Liang L, Chen Z, Dong X et al (2022) Terrestrial mercury and methylmercury bioaccumulation and trophic transfer in subtropical urban forest food webs. Chemosphere 299:134424. https://doi.org/10.1016/j.chemosphere.2022.134424

Zolfaghari G, Esmaili-Sari A, Ghasempouri SM, Baydokhti RR, Hassanzade Kiabi B (2009) A multispecies-monitoring study about bioaccumulation of mercury in Iranian birds (Khuzestan to Persian Gulf): effect of taxonomic affiliation and trophic level. Environ Res 109:830–836. https://doi.org/10.1016/j.envres.2009.07.001